Magnetic Induction-Based Simultaneous Wireless Information and Power Transfer for Single Information and Multiple Power Receivers

Steven Kisseleff, *Student Member, IEEE*, Ian F. Akyildiz, *Fellow, IEEE*, and Wolfgang H. Gerstacker, *Senior Member, IEEE*

***Abstract*— Magnetic induction (MI)-based communication systems have gained increased attention in recent years. Typical applications for these systems lie in the area of wireless power transfer, near-field communication (NFC), and wireless sensor networks in challenging environments. In this paper, a system for simultaneous wireless information and power transfer (SWIPT) using MI-based signal transmission is designed for supporting one data stream and multiple parallel power streams. One of the possible applications for this scheme is an NFC-based access point. The overall system is optimized to guarantee a certain quality-of-service for the data stream as well as a maximum sum receive power for all power receivers (max–sum problem) or a maximum receive power for the worst power receiver (max–min problem), respectively. Both optimization problems turn out to be non-convex, such that the optimum solution cannot be found with limited computational complexity. Hence, we provide efficient suboptimal solutions. In this context, a convex approximation of the transmit power constraint in MI-based multiple-input multiple-output systems turns out to be very useful. A very high achievable power efficiency renders the proposed MI-based SWIPT system very promising.**

***Index Terms*— Magnetic induction, near-field communication, MIMO, SWIPT, wireless communication systems.**

I. Introduction

MAGNETIC induction (MI) based transmission schemes are well known in the context of near-field communication (NFC) [2], wireless power transfer (WPT) [3], and wireless sensor networks (WSN) in challenging environments [4], [5]. In this work, our main focus lies on combining the information transmission with the WPT using resonant coupling of magnetic antennas. Typically, MI based power transfer is only useful within a short range due to a dramatically low power efficiency otherwise, as has been confirmed in numerous previous works (e.g. [3], [6]). Furthermore, the alignment of coils has a strong impact on the transfer efficiency, see e.g. [7], [8]. Several attempts have been made to extend the MI based point-to-point transmission to a system with multiple receivers [9], multiple transmitters [10], or even multiple relays [11], [12]. Moreover, MI based networks with multiple transceivers and relays have been analyzed for the underground WSNs [13]. Finally, the multiple-input multiple-output (MIMO) technique has been introduced for different constellations of MI based communication and WPT systems, see e.g. [14], [15]. In particular, the use of a transmitter equipped with three orthogonally deployed coils is suggested in [15]. This enables a steerable directionality of the resulting magnetic field, the so-called magnetic vector modulation, which is based on the explicit weighting of the field vectors given by the orientations of the transmitter coils [15]. Unfortunately, this approach does not take into account the influence of multiple receivers on each other or on the transmitter. Similarly, in [14], only the carrier frequency is optimized, leaving the choice of e.g. signal phase and amplitude (beamforming coefficients)[1] suboptimal.

Beamforming is a well known technique for maximizing the power efficiency of a MIMO system. In traditional radio frequency (RF) systems, the power efficiency optimization corresponds to the maximization of the receive power for a fixed L_2-norm of the beamforming vector, because the consumed power in the transmitting device depends only on the L_2-norm of the beamforming vector, but not on its particular coefficients. For MI based WPT, the efficiency depends explicitly on the coupling between the transceivers, such that improving the coupling yields an increase of the power efficiency [3]. Furthermore, since the signal reflection is approximately proportional to the squared mutual inductance [16], an influence of the reflected signals on the transmit power is inevitable. In particular, these reflected signals can overlap constructively or destructively depending on the phase of the input signals.

Manuscript received June 20, 2016; revised November 14, 2016; accepted December 24, 2016. Date of publication December 30, 2016; date of current version March 15, 2017. This work has been supported by the German Research Foundation (Deutsche Forschungsgemeinschaft, DFG) under Grant No. GE 861/4-1 and GE 861/4-2 and in part by the US National Science Foundation under the Grant No. 1320758. This paper has been presented in part in the Proceedings of the IEEE GLOBECOM 2015 [1]. The associate editor coordinating the review of this paper and approving it for publication was N. B. Mehta.

S. Kisseleff and W. H. Gerstacker are with the Institute for Digital Communications, Friedrich-Alexander-Universität Erlangen-Nürnberg, Erlangen D-91058, Germany (e-mail: steven.kisseleff@fau.de; wolfgang.gerstacker@fau.de).

I. F. Akyildiz is with the Broadband Wireless Networking Laboratory, School of Electrical and Computer Engineering, Georgia Institute of Technology, Atlanta, GA 30332 USA (e-mail: ian@ece.gatech.edu).

Color versions of one or more of the figures in this paper are available online at http://ieeexplore.ieee.org.

Digital Object Identifier 10.1109/TCOMM.2016.2646684

[1] We follow the literature on WPT using electromagnetic waves [6] and adopt the term beamforming for the optimization of the transmit voltage vector in spatial domain.

Hence, the transmit power depends on the detailed choice of the beamforming coefficients and a sole receive power maximization for a fixed L_2-norm of the beamforming vector becomes insufficient. Therefore, an iterative algorithm has been proposed in [1], which takes into account all couplings and reflections between the coils and maximizes the WPT efficiency. In [1], the overall optimization problem has been shown to be non-convex due to the non-convexity of the transmit power as a function of the beamforming coefficients, such that no globally optimum solution can be found with limited complexity. Hence, an algorithm has been developed which approximates the original optimization problem by a generalized eigenvalue problem in each step of an iterative procedure. In case of convergence, an efficient locally optimal solution has been found.

Simultaneous wireless information and power transfer (SWIPT) is a popular research area, which has been intensely studied in recent years [17]–[20]. Assuming multiple receivers, the power allocation in the transmitter can be optimized in order to enable information broadcasting within a given frequency band to a group of receivers and to efficiently transfer power to the remaining receivers. This can be done using the same transmit signal, such that no switching between data and power transmissions is needed. Despite a significant potential for improvement of the overall system performance, the SWIPT schemes have only been investigated for the RF based communications so far. Due to a much stronger interaction of the magnetic devices in the near-field compared to RF signal transmission and correspondingly a much higher power transfer efficiency, SWIPT schemes seem very promising for near-field applications.

Most of the existing works on SWIPT are related to power allocation and beamforming for multicarrier systems or based on the assumption of flat fading, see, e.g., [17], [20]. As shown in [20] and [21], the optimal power allocation differs substantially for power transfer and information transmission, respectively. From this, a nontrivial tradeoff arises for the system design [21]. However, in MI based communication systems (e.g. NFC), most of the system parameters are selected according to the passive radio frequency identification (RFID, ISO 14443/15693) and NFC (ISO 22536/18000-3) standards, such that the frequency selectivity is very limited. Hence, the optimal resource allocation can be approximated as a uniform power distribution within the utilized transmission band. Therefore, we focus on the beamforming optimization in this work.

We consider one transmitter with three orthogonal coils free of self-interference[2] and multiple single antenna receivers randomly deployed in the near-field of the transmitter. The transmitter can be viewed as an access point, which provides information and/or power upon request. In order to satisfy the needs of the users, we consider two optimization problems for adjusting the system performance according to certain criteria. The first problem is related to the maximization of the sum receive power for all power receivers under a quality-of-service (QoS) constraint for the data receiver. The second problem refers to the maximization of the minimum receive power among all power receivers under the same QoS constraint. Both problems turn out to be non-convex, such that no globally optimum solution can be obtained with a practical approach, and we split each of them into two subproblems, respectively. For the first problem we propose an eigenvalue decomposition and a gradient based search. The second problem is reformulated into a semidefinite program with relaxation of a rank-1 constraint followed by randomization and a gradient based search. In addition, the non-convex transmit power constraint is revealed. In order to incorporate this constraint into the considered optimization problems, two strategies have been investigated. The corresponding non-convex transmit power metric is replaced by either a squared L_2-norm of the beamforming vector (far-field approximation) or taken into account by using an iterative convex approximation (proposed solution). In this context, substantial receive power gains have been observed using the proposed solution compared to the traditional far-field approximation, which render the considered MI based SWIPT system very power efficient and promising.

Our contribution can be summarized as follows:

- A novel MI based SWIPT system is proposed and the key aspects of its design and optimization are investigated;
- an iterative convex approximation strategy is introduced and adopted for the system optimization with respect to two typical performance metrics;
- the considerable potential of the proposed SWIPT scheme is revealed.

This paper is organized as follows. Section II provides insight into the system model for MI based SWIPT with three transmission coils and multiple receivers. In Section III-A, the two constrained optimization problems are formulated. Then, the baseline solutions using far-field approximation are discussed in Section III-B. The proposed iterative convex approximation strategy is presented in Section III-C and applied to the mentioned optimization problems in Section III-D. In Section IV, numerical results are discussed, and Section V concludes the paper.

II. System Model

In this work, we assume a system with one transmitter equipped with three orthogonally deployed coils (3D-coil) and multiple (K) receivers with one coil each, see Fig. 1. Furthermore, in order to establish a SWIPT scheme, we assume that one of the users receives information (we call this user a data receiver (DR)), whereas all other users receive power (we call these users power receivers (PRs)). Every transmitter coil has inductivity L_t and is considered as part of a transmitter resonant circuit, which includes also a capacitor with capacitance C_t and a resistor with resistance R_t (modeling the copper resistance of the coil). Similarly, the

[2]In a practical system, the assumed orthogonality of the coils may not be exact, such that non-vanishing self-interference signals (cross-talk) would occur and affect the system behavior. Interestingly, the resulting correlation of the transmit signals would make the considered baseline scheme (see Section III-B) even less efficient. On the other hand, these imperfections can be measured and taken into account in the proposed scheme, see Section III-D, such that the system performance would not differ much.

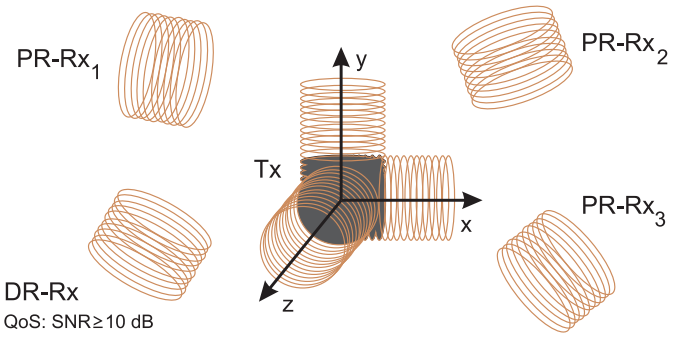

Fig. 1. Example of a SWIPT system with 3D-coil based transmitter (Tx) and multiple ($K = 4$) single coil receivers (three power receivers (PRs) ($\mathrm{PR}-\mathrm{Rx}_1$, $\mathrm{PR}-\mathrm{Rx}_2$, and $\mathrm{PR}-\mathrm{Rx}_3$) and one data receiver ($\mathrm{DR}-\mathrm{Rx}$) with a QoS (signal-to-noise ratio (SNR)) constraint).

receiver resonance circuit includes a coil with inductivity L_r, a capacitor with capacitance C_r and a resistor with resistance R_r. Both capacitances C_t and C_r are selected to make the respective circuits resonant at the resonance frequency f_0 using the relation $f_0 = \frac{1}{2\pi\sqrt{L_t C_t}} = \frac{1}{2\pi\sqrt{L_r C_r}}$.

Since the considered system can be viewed as a variation of the traditional NFC and passive RFID based systems, we select the commonly used resonance frequency $f_0 = 13.56$ MHz and a bandwidth $B = 14$ kHz for all numerical results. For these values, the frequency selectivity of the transmission channel is typically very low even for large quality factors (e.g. above 100) of the resonant circuits and not too high coupling coefficients (e.g. below 0.1). Such channels do not need any extensive equalization or frequency-selective prefiltering (precoding). However, in case of very strong couplings between the coils, the well-known effect of frequency-splitting occurs [22], which can make the transmission channel frequency-selective. Therefore, in order to provide a general approach for all types of channels (weak coupling and strong coupling), we must assume a non-vanishing frequency selectivity of the transmission channels. Correspondingly, the data receiver employs a linear filter, in order to remove the resulting intersymbol interference and equalize the channel. This filtering at the receiver seems to be sufficient for coping with the frequency selectivity of the transmission channel, such that the transmit filter does not need to be frequency-selective as well. Hence, a frequency-flat transmit filter is utilized in the following.

Each receiver circuit contains an additional real-valued load resistor Z_L. Hence, the inner impedance of each transmitter circuit can be given by

$$Z_{\mathrm{in},t}(f) = j2\pi f L_t + \frac{1}{j2\pi f C_t} + R_t, \tag{1}$$

and for the inner impedance of each receiver circuit

$$Z_{\mathrm{in},r}(f) = j2\pi f L_r + \frac{1}{j2\pi f C_r} + R_r + Z_L \tag{2}$$

is valid. A single transmitter-receiver link is shown in Fig. 2. The load impedance is optimized according to previous works, cf. [3]. The induced voltage is related to the coupling

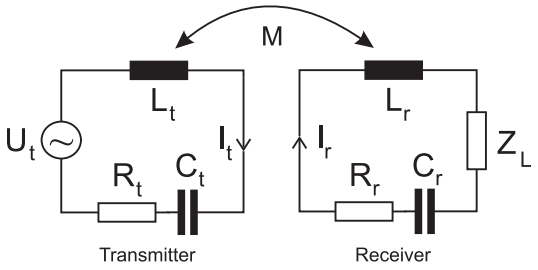

Fig. 2. A single MI link. Transmitter and receiver resonance circuits.

between the coils, which is determined by the mutual inductance M. With the knowledge of the mutual inductance M, the frequency selectivity of the MI channel is entirely known, such that not only the WPT can be established but also the information transmission [23].

The orientations and alignments of the coupled coils have a strong impact on the mutual inductance and correspondingly on the path loss, cf. [8]. Hence, we model the mutual inductance between any two coils m and l of the coupled network by

$$M_{m,l} = \overline{M}_{m,l} \cdot J_{m,l}, \tag{3}$$

$$J_{m,l} = 2\sin\theta_m \sin\theta_l + \cos\theta_m \cos\theta_l \cos\phi, \tag{4}$$

cf. [13], where θ_m and θ_l are the angles between the radial directions of the coils m and l, respectively, and the line connecting the two coil centers. ϕ is the angle difference between the coils' axes in the plane, which is orthogonal to the direction of transmission. $\overline{M}_{m,l}$ represents the (absolute) value of the mutual inductance for the case $J_{m,l} = 1$. For the subsequent derivations, we define $Z_{m,l}(f) = j2\pi f M_{m,l}$, $\forall m \neq l$.

In the following, $(\cdot)^T$ and $(\cdot)^H$ stand for transpose and Hermitian transpose, respectively. Furthermore, the rank and the trace of a matrix are denoted by $\mathrm{rank}(\cdot)$ and $\mathrm{tr}\{\cdot\}$, respectively. In addition, the positive-semidefiniteness of a matrix is expressed by "$\succeq 0$". For simplicity, we assign the first three indices $m \in \{1, 2, 3\}$ to the transmitter circuits and the remaining indices $m \in \{4, \ldots, K+3\}$ to the receiver circuits, respectively.

For the signal transmission, we assume a concatenation of a transmit filter with an impulse response $h(t)$ in time domain and a beamforming filter $\mathbf{b} = [b_1, b_2, b_3]^T$ in spatial domain. Thus, a sequence of statistically independent transmit symbols $s[n]$ spaced by symbol duration $T = 1/B$ (with bandwidth B) is fed into the transmit filter $h(t)$ and then mapped onto three transmit voltages using the beamforming filter $\mathbf{b}$, which generates the voltage signals $u_m(t)$, $m \in \{1, 2, 3\}$ in all three resonance circuits. Furthermore, we assume that $\mathcal{E}\{|s[n]|^2\} = 1$, where $\mathcal{E}\{\cdot\}$ denotes the expectation operator. In time domain, the complex-valued transmit voltage of circuit m is given by

$$u_m(t) = b_m \sum_{n=-\infty}^{\infty} s[n]h(t - nT), \quad m \in \{1, 2, 3\}. \tag{5}$$

In frequency domain, we consider the complex-valued amplitudes $U_m(f) = \mathcal{F}\{u_m(t)\}$ and $I_m(f) = \mathcal{F}\{i_m(t)\}$ of the voltages $u_m(t)$ and currents $i_m(t)$, respectively, of the mth circuit. Here, $\mathcal{F}\{\cdot\}$ denotes the Fourier transform operator.

For simplicity, we assume a frequency-flat filter characteristic within the bandwidth of the filter, which corresponds to a root-raised cosine (RRC) impulse response $h(t)$ with roll-off factor $\beta = 0$ and Fourier transform

$$H(f) = \begin{cases} \dfrac{1}{B}, & f_0 - 0.5B \le f \le f_0 + 0.5B, \\ 0, & \text{else.} \end{cases} \tag{6}$$

In order to determine the average power density spectrum of the transmit signal, we consider the Fourier transform $U_m(f)$ of a transmit signal comprising N_{sym} transmit symbols according to (5),

$$U_m(f) = b_m \frac{1}{B} \sum_{n=0}^{N_{sym}-1} s[n]\, \mathrm{e}^{-j2\pi f n T}, \qquad f_0 - 0.5B \le f \le f_0 + 0.5B. \tag{7}$$

The corresponding average power density spectrum of the transmit signal in circuit m is obtained as (cf. [24] and [25])

$$\begin{aligned} &\lim_{N_{sym}\to\infty} \frac{B}{N_{sym}}\, \mathcal{E}\{|U_m(f)|^2\} \\ &\quad = \lim_{N_{sym}\to\infty} \frac{B}{N_{sym}} \frac{|b_m|^2\, N_{sym}}{B^2} \\ &\quad = |b_m|^2 \frac{1}{B}, \quad f_0 - 0.5B \le f \le f_0 + 0.5B, \end{aligned} \tag{8}$$

where $\lim_{\{\cdot\}}$ denotes the limit operator. For each circuit m, the current amplitude $I_m(f)$ depends on the current amplitudes $I_l(f)$, $\forall l \neq m$ in all surrounding circuits via the voltage equation

$$I_m(f) \cdot Z_{\mathrm{in},t}(f) + \sum_{l \neq m} \big(I_l(f) \cdot Z_{m,l}(f)\big) = U_m(f), \tag{9}$$

if m belongs to a transmitter or

$$I_m(f) \cdot Z_{\mathrm{in},r}(f) + \sum_{l \neq m} \big(I_l(f) \cdot Z_{m,l}(f)\big) = 0, \tag{10}$$

if m belongs to a receiver. In (10), $U_m(f) = 0$ and correspondingly $u_m(t) \equiv 0$ holds, since only the transmitter is supposed to generate power. In order to calculate the currents in all circuits of the coupled network, a set of voltage equations

$$\begin{bmatrix} \mathbf{Z}_{Tx}(f) & \mathbf{Z}_{Ch}(f) \\ \mathbf{Z}_{Ch}^T(f) & \mathbf{Z}_{Rx}(f) \end{bmatrix} \cdot \begin{bmatrix} \mathbf{I}_{Tx}(f) \\ \mathbf{I}_{Rx}(f) \end{bmatrix} = \begin{bmatrix} \mathbf{U}_{Tx}(f) \\ \mathbf{0} \end{bmatrix} \tag{11}$$

needs to be solved. Here, $\mathbf{U}_{Tx}(f) = [U_1(f), U_2(f), U_3(f)]^T$ is the complex-valued input voltage vector at the transmitter. Furthermore, $\mathbf{0}$ stands for an all-zero vector of dimension $K \times 1$. $\mathbf{I}_{Tx}(f)$ and $\mathbf{I}_{Rx}(f)$ denote vectors comprising the complex-valued currents of the transmitter and the receiver circuits, respectively. The matrices $\mathbf{Z}_{Tx}(f)$, $\mathbf{Z}_{Ch}(f)$ and $\mathbf{Z}_{Rx}(f)$ contain complex impedances and are defined in the following. In this work, we use a 3D-coil based transmitter, which means that all three transmitter coils' axes are orthogonal to each other, such that

$$\begin{aligned} \mathbf{Z}_{Tx}(f) &= \begin{bmatrix} Z_{\mathrm{in},t}(f) & 0 & 0 \\ 0 & Z_{\mathrm{in},t}(f) & 0 \\ 0 & 0 & Z_{\mathrm{in},t}(f) \end{bmatrix} \\ &= Z_{\mathrm{in},t}(f) \cdot \mathbf{I}_3 \end{aligned} \tag{12}$$

holds, where $\mathbf{I}_3$ stands for the identity matrix of dimension 3×3. The receiver coils are not necessarily orthogonal to each other and we obtain

$$\mathbf{Z}_{Rx}(f) = \begin{bmatrix} Z_{\mathrm{in},r}(f) & \cdots & Z_{K+3,4}(f) \\ \vdots & \ddots & \vdots \\ Z_{4,K+3}(f) & \cdots & Z_{\mathrm{in},r}(f) \end{bmatrix}. \tag{13}$$

The purely imaginary matrices $\mathbf{Z}_{Ch}(f)$ and $\mathbf{Z}_{Ch}^T(f)$ in (11) stand for the influence of the receiver coils onto the transmitter coils and vice versa, respectively. Hence, $\mathbf{Z}_{Ch}(f)$ is defined by

$$\mathbf{Z}_{Ch}(f) = \begin{bmatrix} Z_{4,1}(f) & Z_{5,1}(f) & \cdots & Z_{K+3,1}(f) \\ Z_{4,2}(f) & Z_{5,2}(f) & \cdots & Z_{K+3,2}(f) \\ Z_{4,3}(f) & Z_{5,3}(f) & \cdots & Z_{K+3,3}(f) \end{bmatrix}. \tag{14}$$

By inverting the overall impedance matrix in (11) using [26], we obtain similar to [9]

$$\begin{aligned} \mathbf{I}_{Tx}(f) &= \Big(\mathbf{Z}_{Tx}(f) - \mathbf{Z}_{Ch}(f)\mathbf{Z}_{Rx}^{-1}(f)\mathbf{Z}_{Ch}^T(f)\Big)^{-1} \mathbf{U}_{Tx}(f) \\ &= \mathbf{A}(f)\mathbf{U}_{Tx}(f), \end{aligned} \tag{15}$$

$$\begin{aligned} \mathbf{I}_{Rx}(f) &= -\mathbf{Z}_{Rx}^{-1}(f)\mathbf{Z}_{Ch}^T(f)\mathbf{A}(f)\mathbf{U}_{Tx}(f) \\ &= \mathbf{C}(f)\mathbf{U}_{Tx}(f), \end{aligned} \tag{16}$$

with implicit definitions of $\mathbf{A}(f)$ and $\mathbf{C}(f)$. In addition, we define[3]

$$\mathbf{D}(f) = \Big(\mathbf{Z}_{Rx}(f) - \mathbf{Z}_{Ch}^T(f)\mathbf{Z}_{Tx}^{-1}(f)\mathbf{Z}_{Ch}(f)\Big)^{-1}, \tag{17}$$

which will be discussed in the context of noise power calculation.

As known from the fundamentals of electric power generation and transmission (e.g. [27], [28]), in order to produce enough active power in electric circuits, the transmitter/generator needs to release also the reactive power, which corresponds to the imaginary part of the generated complex power $\int_{f_0-0.5B}^{f_0+0.5B} \lim_{N_{sym}\to\infty} \frac{B}{N_{sym}}\, \mathcal{E}\{U_m(f) I_m(f)\}\, \mathrm{d}f$, $m \in \{1, 2, 3\}$. The reactive power is not absorbed by the load, but fluctuates between the power source and the load impedance. Furthermore, without the reactive power, the induction coils cannot be operated. However, a large amount of reactive power might limit the performance of the communication system and impose additional hard constraints for the system design. This problem has been explicitly addressed in [29], where the reactive power for an MI based WPT system has been minimized under the active receive power constraints. Unfortunately, this approach does not necessarily maximize the power efficiency of the system, since the active transmit power may dominate the reactive transmit power in some cases. Correspondingly, if not incorporated into the WPT optimization, the active transmit power may become very large and dramatically reduce the transfer efficiency. Hence, both real and imaginary parts of the transmit power need to be taken into account, such that the magnitude of the total generated complex power (the so-called apparent power [28]) is a better reference for the transmit power than the pure active [3] or

[3]Matrix $\mathbf{D}(f)$ is used in order to describe the influence of the noise voltages in the receiver circuits on the currents in the receiver circuits similarly to the matrix $\mathbf{C}(f)$, which maps the signals from the transmitter circuits onto the currents in the receiver circuits.

$$
\begin{aligned}
P_{t,\text{total}} &= \sum_{m=1}^{3} \int_{f_0-0.5B}^{f_0+0.5B} P_{t,m}(f)\,\mathrm{d}f \\
&= \int_{f_0-0.5B}^{f_0+0.5B} \lim_{N_{sym}\to\infty} \frac{B}{N_{sym}}\, \mathcal{E}\{|\mathbf{U}_{Tx}(f)|^T\, |\mathbf{A}(f)\mathbf{U}_{Tx}(f)|\}\,\mathrm{d}f \\
&= \int_{f_0-0.5B}^{f_0+0.5B} \lim_{N_{sym}\to\infty} \frac{B}{N_{sym}}\, \mathcal{E}\left\{ \left| \mathbf{b}\,\frac{1}{B} \sum_{n=0}^{N_{sym}-1} s[n]\,\mathrm{e}^{-j2\pi f n T} \right|^T \left| \mathbf{A}(f)\mathbf{b}\,\frac{1}{B} \sum_{n=0}^{N_{sym}-1} s[n]\,\mathrm{e}^{-j2\pi f n T} \right| \right\} \mathrm{d}f \\
&= \int_{f_0-0.5B}^{f_0+0.5B} \lim_{N_{sym}\to\infty} \frac{B}{N_{sym}}\, \mathcal{E}\left\{ \left| \frac{1}{B} \sum_{n=0}^{N_{sym}-1} s[n]\,\mathrm{e}^{-j2\pi f n T} \right|^2 \right\} |\mathbf{b}|^T\, |\mathbf{A}(f)\mathbf{b}|\,\mathrm{d}f \\
&= \frac{1}{B} \int_{f_0-0.5B}^{f_0+0.5B} |\mathbf{b}|^T\, |\mathbf{A}(f)\mathbf{b}|\,\mathrm{d}f, \qquad (19)
\end{aligned}
$$

reactive [29] power. The apparent transmit power spectral density in the mth transmitter circuit is given by

$$
\begin{aligned}
P_{t,m}(f) &= \lim_{N_{sym}\to\infty} \frac{B}{N_{sym}}\, \mathcal{E}\{|U_m(f) I_m(f)|\} \\
&= \lim_{N_{sym}\to\infty} \frac{B}{N_{sym}}\, \mathcal{E}\{|U_m(f)|\,|I_m(f)|\}, \qquad (18)
\end{aligned}
$$

where $|\cdot|$ denotes the element-wise absolute value operator. Therefore, we define the total power provided by the transmitter within a given transmission band with center frequency f_0 and bandwidth B as $P_{t,\text{total}}$ given in (19), as shown at the top of this page, where (15), (7), and (8) have been used. For weak couplings between coils (low mutual inductance), matrix $\mathbf{A}(f)$ is approximately[4] given by

$$
\mathbf{A}(f) \approx \mathbf{Z}_{Tx}^{-1}(f) = Z_{\text{in},t}^{-1}(f) \cdot \mathbf{I}_3. \qquad (20)
$$

This yields

$$
P_{t,\text{total}} \approx \mathbf{b}^H \mathbf{b}\,\frac{1}{B} \int_{f_0-0.5B}^{f_0+0.5B} \left| Z_{\text{in},t}^{-1}(f) \right| \mathrm{d}f. \qquad (21)
$$

This result motivates the use of a far-field approximation, where the transmit power is only related to the squared L_2-norm of $\mathbf{b}$. However, in case of strong couplings between coils (or imperfect coil deployment at the transmitter), this approximation is not valid, which may lead to a performance degradation.

For the received active power density at the load resistor Z_L of the receiver circuit $l \in \{4, \ldots, K+3\}$ we obtain

$$
\begin{aligned}
P_{r,l}(f) &= \lim_{N_{sym}\to\infty} \frac{B}{N_{sym}}\, \mathcal{E}\{|I_l(f)|^2\} Z_L \\
&= \lim_{N_{sym}\to\infty} \frac{B}{N_{sym}}\, \mathcal{E}\{\left| \mathbf{e}_{K,l-3}^H \mathbf{C}(f) \mathbf{U}_{Tx}(f) \right|^2\} Z_L \\
&= \frac{1}{B} \mathbf{b}^H \mathbf{C}^H(f) \mathbf{e}_{K,l-3} \mathbf{e}_{K,l-3}^H \mathbf{C}(f) \mathbf{b} Z_L, \qquad (22)
\end{aligned}
$$

where the $K \times 1$ vector $\mathbf{e}_{K,l}$ is defined as $\mathbf{e}_{K,l} = [0, \ldots, 0, 1, 0, \ldots, 0]^T$ with the '1' at the lth position, and (16) has been used. In case of power transfer, the total receive power at circuit l is given by

$$
\begin{aligned}
&P_{r,l,\text{total}} \\
&\quad = \eta \int_{f_0-0.5B}^{f_0+0.5B} P_{r,l}(f)\,\mathrm{d}f \\
&\quad = \mathbf{b}^H \left(\frac{\eta Z_L}{B} \int_{f_0-0.5B}^{f_0+0.5B} \mathbf{C}^H(f) \mathbf{e}_{K,l-3} \mathbf{e}_{K,l-3}^H \mathbf{C}(f) \mathrm{d}f \right) \mathbf{b}, \qquad (23)
\end{aligned}
$$

where η stands for the losses due to the conversion of the received high frequency signals into electric power. For simplicity, we assume $\eta = 1$ in this work.

In case of information transmission, the transmitted data may be corrupted by noise and interference caused by other systems (in particular by other MI based transmissions). We model the noise source in each resonant circuit as a voltage source, which provides an additive white Gaussian noise (AWGN) with the average power spectral density (PSD) N_0. The uncorrelated noise signals may occur in all resonant circuits (including the receiver circuit). These signals influence not only the currents in the respective circuits, but also the currents of the neighboring circuits via near-field coupling between the coils. Hence, the additive noise power as seen by the receiver l can be calculated via summation of the active received noise powers from all noise sources of the system. Considering the Fourier transform $U_{N,m}(f) = \int_0^{N_{sym}/B} u_{N,m}(t)\,\mathrm{e}^{-j2\pi f t}\,\mathrm{d}t$ of the noise signal $u_{N,m}(t)$ in circuit m within a time window, where N_{sym}/B is the window width, we obtain $\lim_{N_{sym}\to\infty} \frac{B}{N_{sym}} \mathcal{E}\{\left|U_{N,m}(f)\right|^2\} = N_0$, $\forall m$, see e.g. [25]. The current in the lth receiver can be expressed as

$$
\begin{aligned}
I_l(f) = &\sum_{m=1}^{3} \mathbf{e}_{K,l-3}^H \mathbf{C}(f) \mathbf{e}_{3,m} U_{N,m}(f) \\
&+ \sum_{m=4}^{K+3} \mathbf{e}_{K,l-3}^H \mathbf{D}(f) \mathbf{e}_{K,m-3} U_{N,m}(f). \qquad (24)
\end{aligned}
$$

[4]For $\left(2\pi f \max_{m,l}\{\overline{M}_{m,l}\} \ll R\right)$, $\mathbf{Z}_{Ch}(f)\mathbf{Z}_{Rx}^{-1}(f)\mathbf{Z}_{Ch}^T(f)$ in (15) is negligible.

$$
\begin{aligned}
N_l(f) &= \lim_{N_{sym}\to\infty} \frac{B}{N_{sym}}\, \mathcal{E}\left\{ \left| \sum_{m=1}^{3} \mathbf{e}_{K,l-3}^H \mathbf{C}(f)\mathbf{e}_{3,m} U_{N,m}(f) \right|^2 + \left| \sum_{m=4}^{K+3} \mathbf{e}_{K,l-3}^H \mathbf{D}(f)\mathbf{e}_{K,m-3} U_{N,m}(f) \right|^2 \right\} Z_L \\
&= \lim_{N_{sym}\to\infty} \frac{B}{N_{sym}}\, \mathbf{e}_{K,l-3}^H \mathbf{C}(f)\, \mathcal{E}\left\{ \sum_{m=1}^{3} \mathbf{e}_{3,m} \left| U_{N,m}(f) \right|^2 \mathbf{e}_{3,m}^H \right\} \mathbf{C}^H(f)\mathbf{e}_{K,l-3} Z_L \\
&\quad + \lim_{N_{sym}\to\infty} \frac{B}{N_{sym}}\, \mathbf{e}_{K,l-3}^H \mathbf{D}(f) \mathcal{E}\left\{ \sum_{m=4}^{K+3} \mathbf{e}_{K,m-3} \left| U_{N,m}(f) \right|^2 \mathbf{e}_{K,m-3}^H \right\} \mathbf{D}^H(f)\mathbf{e}_{K,l-3} Z_L \\
&= N_0 \mathbf{e}_{K,l-3}^H \mathbf{C}(f)\mathbf{C}^H(f)\mathbf{e}_{K,l-3} Z_L + N_0 \mathbf{e}_{K,l-3}^H \mathbf{D}(f)\mathbf{D}^H(f)\mathbf{e}_{K,l-3} Z_L \\
&= N_0 \mathbf{e}_{K,l-3}^H \left(\mathbf{C}(f)\mathbf{C}^H(f) + \mathbf{D}(f)\mathbf{D}^H(f) \right) \mathbf{e}_{K,l-3} Z_L, \qquad (25)
\end{aligned}
$$

The corresponding average received noise PSD $N_l(f) = \lim_{N_{sym}\to\infty} \frac{B}{N_{sym}}\, \mathcal{E}\{|I_l(f)|^2\} Z_L$ can be therefore given by (25), as shown at the top of this page, where $\sum_{m=1}^{K} \mathbf{e}_{K,m}\mathbf{e}_{K,m}^H = \mathbf{I}_K$ has been used. Obviously, the resulting noise PSD is not white anymore. Therefore, we employ a whitening filter $H_{w,l}(f) = \sqrt{\frac{1\,V^2 s}{N_l(f) Z_L}}$ in the lth receiver,[5] which completely removes the frequency selectivity of the noise. Furthermore, a linear equalizer (LE) is utilized at the receiver, which minimizes the mean-squared error (MSE) of the equalized signal (minimum MSE, MMSE). As known from the literature (cf. [30]), the resulting signal-to-noise ratio (SNR) at the output of the unbiased MMSE-LE can be written as[6]

$$
\begin{aligned}
&\mathrm{SNR}_l \\
&= \left(\frac{1}{B} \int_{f_0-0.5B}^{f_0+0.5B} \frac{\mathrm{d}f}{\frac{P_{r,l}(f) Z_L}{1V^2 s} \left| H_{w,l}(f) \right|^2 + 1} \right)^{-1} - 1 \\
&= \left(\int_{f_0-0.5B}^{f_0+0.5B} \frac{\frac{1}{B}\,\mathrm{d}f}{\frac{\frac{1}{B}\mathbf{b}^H \mathbf{C}^H(f)\mathbf{e}_{K,l-3}\mathbf{e}_{K,l-3}^H \mathbf{C}(f)\mathbf{b}}{N_0 \mathbf{e}_{K,l-3}^H (\mathbf{C}(f)\mathbf{C}^H(f) + \mathbf{D}(f)\mathbf{D}^H(f))\mathbf{e}_{K,l-3}} + 1} \right)^{-1} - 1. \qquad (26)
\end{aligned}
$$

In order to ensure a reliable signal detection at the receiver l, a typical QoS constraint is imposed. For our numerical results, we demand that $\mathrm{SNR}_l \geq \mathrm{SNR}_{thr}$, where $\mathrm{SNR}_{thr} = 10$ dB is assumed to be sufficient for the target application.

III. MI Based SWIPT

In this section, two optimization problems related to the design of an MI based SWIPT system are discussed.

A. Problem Formulation

Different optimization problems have been discussed in the literature in the context of SWIPT systems for traditional RF communication, cf. e.g. [17], [21]. We consider a SWIPT system with a single DR that is intended to receive an information stream with a given QoS and multiple PRs that are intended to receive power. In the following, two optimization problems are presented. The first problem refers to the maximization of the sum receive power among all PRs[7] under a given QoS constraint and a transmit power constraint. It can be formulated as follows:

$$
\begin{aligned}
\text{Max} - \text{sum problem}: \ &\max_{\mathbf{b}} \sum_{l=4, l\neq\kappa}^{K+3} P_{\mathrm{r},l,\mathrm{total}}, \\
&\text{s.t.: } \mathrm{SNR}_\kappa \geq \mathrm{SNR}_{thr}, \qquad (27) \\
&P_{t,\mathrm{total}} \leq P,
\end{aligned}
$$

where receiver κ has been selected for data reception with a QoS given by SNR_{thr}.

The second optimization problem refers to the maximization of the minimum received power among all PRs under the same constraints as in (27). It can be formulated as follows:

$$
\begin{aligned}
\text{Max} - \text{min problem}: \ &\max_{\mathbf{b}} \min_{4\leq l\leq K+3, l\neq\kappa} P_{\mathrm{r},l,\mathrm{total}}, \\
&\text{s.t.: } \mathrm{SNR}_\kappa \geq \mathrm{SNR}_{thr}, \\
&P_{t,\mathrm{total}} \leq P. \qquad (28)
\end{aligned}
$$

Both optimization problems are non-convex due to the non-convex constraints, which can be shown by inspecting (19) which is related to the transmit power constraint and (26) combined with the observations from [31] for the QoS constraint. Therefore, the well-known tools of convex optimization [32] are not applicable. Except for the transmit power constraint, the optimization problems (27) and (28) do not differ much from the traditional beamforming problems known from the fundamentals of communications and MIMO systems (cf. [33]), where, however, the transmit power constraint is convex. In Section III-B, the problems (27) and (28) are simplified via the approximation of the transmit power (19) by a squared L_2-norm of the beamforming vector. This approximation is valid for all types of far-field communications. Hence, the corresponding simplified optimization problems can be viewed as traditional beamforming problems and are related to baseline schemes that we use for performance

[5]The noise PSD needs to be multiplied with Z_L, since the whitening filter is applied to a voltage signal. Hence, a unitless filter results.

[6]For the correct calculation, $\frac{P_{r,l}(f) Z_L}{1V^2 s}$ represents the unitless power density of the received signal at frequency f.

[7]The priority based maximization of the receive power can be done by introducing additional weights (priorities) λ_l in the sum in (27), which can be absorbed into the respective receive powers $P_{\mathrm{r},l,\mathrm{total}}$. Hence, the optimization strategies described below may be applied to the priority based SWIPT as well.

comparisons. However, the resulting optimized beamforming vectors provide only strictly suboptimum solutions to the original problem formulations (27) and (28), if the devices are in the near-field of the transmitter. Hence, a more precise convex approximation of the transmit power constraint is provided in Section III-C. This approximation is combined with the approach from Section III-B in each iteration of an iterative algorithm proposed in Section III-D.

B. Far-Field Approximation

1) Max-Sum Problem: We consider an optimization problem, which is identical to (27) except for the transmit power constraint:

$$\begin{aligned}&\max_{\mathbf{b}}\ \mathbf{b}^H\left(\sum_{\substack{l=4,\\ l\neq\kappa}}^{K+3}\int_{f_0-0.5B}^{f_0+0.5B}\mathbf{C}^H(f)\mathbf{e}_{K,l-3}\mathbf{e}_{K,l-3}^H\mathbf{C}(f)\mathrm{d}f\right)\mathbf{b},\\ &\text{s.t.:}\left(\int_{f_0-0.5B}^{f_0+0.5B}\frac{\frac{1}{B}\,\mathrm{d}f}{\frac{\frac{1}{B}\mathbf{b}^H\mathbf{C}^H(f)\mathbf{e}_{K,\kappa-3}\mathbf{e}_{K,\kappa-3}^H\mathbf{C}(f)\mathbf{b}}{N_0\mathbf{e}_{K,\kappa-3}^H(\mathbf{C}(f)\mathbf{C}^H(f)+\mathbf{D}(f)\mathbf{D}^H(f))\mathbf{e}_{K,\kappa-3}}+1}\right)^{-1}-1\\ &\quad\geq \mathrm{SNR}_{thr},\\ &\quad\mathbf{b}^H\mathbf{b}\leq P_0,\end{aligned}\tag{29}$$

where P_0 is a properly chosen constant[8] related to the transmit power P. The matrices $\mathbf{C}(f)$, $\mathbf{D}(f)$ and the vector $\mathbf{b}$ have been defined in Section II. Unfortunately, due to the QoS constraint, a traditional approach, e.g. based on semidefinite relaxation (SDR) or eigenvalue decomposition, cannot be applied, cf. [31], [34]. Therefore, we decompose (29) into two subproblems, where the first subproblem refers to the maximization of the receive power under only the transmit power constraint and the second subproblem is related to the QoS constraint and the gradient based search. The first subproblem can be formulated similarly to (29) as

$$\begin{aligned}&\max_{\mathbf{b}}\ \mathbf{b}^H\mathbf{W}_{\mathrm{sum}}\mathbf{b},\\ &\text{s.t.: }\mathbf{b}^H\mathbf{b}\leq P_0,\end{aligned}\tag{30}$$

with

$$\mathbf{W}_{\mathrm{sum}}=\sum_{l=4,\ l\neq\kappa}^{K+3}\int_{f_0-0.5B}^{f_0+0.5B}\mathbf{C}^H(f)\mathbf{e}_{K,l-3}\mathbf{e}_{K,l-3}^H\mathbf{C}(f)\mathrm{d}f.\tag{31}$$

Obviously, (30) is an eigenvalue problem and can be solved by selecting the (properly scaled) eigenvector of $\mathbf{W}_{\mathrm{sum}}$, which pertains to the maximum eigenvalue. If the solution does not satisfy the QoS constraint, a gradient based approach from [31] is utilized, in order to increase the value of SNR_κ, until the QoS requirement is fulfilled. The gradient based algorithm is described via pseudo code notation in Algorithm 1. In each

[8]The value for P_0 corresponds to $P\Big/\left(\frac{1}{B}\int_{f_0-0.5B}^{f_0+0.5B}\left|Z_{\mathrm{in},t}^{-1}(f)\right|\mathrm{d}f\right)$, as can be deduced from (21).

Algorithm 1 Gradient Based Improvement of SNR_κ

Input: $\mathbf{b}_1$
Calculate SNR_κ;
$i=1$, $\mathbf{b}_0=\mathbf{0}$;
while ($\mathrm{SNR}_\kappa<\mathrm{SNR}_{thr}$) & $\left(1-\frac{|\mathbf{b}_{i-1}^H\mathbf{b}_i|}{|\mathbf{b}_{i-1}|^T|\mathbf{b}_i|}\geq\epsilon\right)$ **do**
  Calculate $grad_i\{\mathrm{SNR}_\kappa\}$ from (32) using $\mathbf{b}_i$;
  Select δ_i according to [30];
  Update $\mathbf{b}_{i+1}=\mathbf{b}_i+\delta_i\cdot grad_i\{\mathrm{SNR}_\kappa\}$;
  Normalize $\mathbf{b}_{i+1}\Rightarrow P_{t,\mathrm{total}}=P$;
  Calculate SNR_κ;
  Update $i=i+1$;
end while
Output: $\mathbf{b}_i$.

iteration i of the gradient search, the direction[9] of the gradient is determined via [31]

$$\begin{aligned}&grad_i\{\mathrm{SNR}_\kappa\}\\ &=\left(\int_{f_0-0.5B}^{f_0+0.5B}\frac{\frac{1}{B^2}\mathbf{C}^H(f)\mathbf{e}_{K,\kappa-3}\mathbf{e}_{K,\kappa-3}^H\mathbf{C}(f)}{N_0\mathbf{e}_{K,\kappa-3}^H(\mathbf{C}(f)\mathbf{C}^H(f)+\mathbf{D}(f)\mathbf{D}^H(f))\mathbf{e}_{K,\kappa-3}}\,\mathrm{d}f}{\left(\frac{\frac{1}{B}\mathbf{b}_i^H\mathbf{C}^H(f)\mathbf{e}_{K,\kappa-3}\mathbf{e}_{K,\kappa-3}^H\mathbf{C}(f)\mathbf{b}_i}{N_0\mathbf{e}_{K,\kappa-3}^H(\mathbf{C}(f)\mathbf{C}^H(f)+\mathbf{D}(f)\mathbf{D}^H(f))\mathbf{e}_{K,\kappa-3}}+1\right)^2}\right)\mathbf{b}_i,\end{aligned}\tag{32}$$

where $\mathbf{b}_i$ denotes the state of the vector $\mathbf{b}$ in the beginning of the ith iteration. The iteration consists of an update step

$$\mathbf{b}_{i+1}=\mathbf{b}_i+\delta_i\cdot grad_i\{\mathrm{SNR}_\kappa\}\tag{33}$$

and an evaluation step, where the value of SNR_κ is calculated and compared with SNR_{thr}. If the QoS constraint is fulfilled, the algorithm stops and the sum receive power corresponding to the obtained beamforming vector is calculated. If $\mathbf{b}_i$ and $\mathbf{b}_{i-1}$ are very similar (i.e., if $1-\frac{|\mathbf{b}_{i-1}^H\mathbf{b}_i|}{|\mathbf{b}_{i-1}|^T|\mathbf{b}_i|}<\epsilon$ holds with a sufficiently small ϵ, e.g. $\epsilon=10^{-3}$) and $\mathrm{SNR}_\kappa<\mathrm{SNR}_{thr}$, we assume that a local maximum has been reached, while the QoS constraint remains unfulfilled. Hence, in this case, the algorithm stops and a failure is reported. The choice of the step size δ_i is important for the system performance as well. We follow the recommendations provided in [30] and select the step size accordingly.

2) Max-Min Problem: Similarly to the max-sum problem, the maximization of the minimum receive power according to (28) with a simplified transmit power constraint can be

[9]The true value of the gradient corresponds to $grad_i\{\mathrm{SNR}_\kappa\}$ from (32) multiplied with a scalar factor $\left(\frac{1}{B}\int_{f_0-0.5B}^{f_0+0.5B}\frac{1}{\frac{\mathbf{b}_i^H\mathbf{C}^H(f)\mathbf{e}_{K,\kappa-3}\mathbf{e}_{K,\kappa-3}^H\mathbf{C}(f)\mathbf{b}_i}{BN_0\mathbf{e}_{K,\kappa-3}^H\left(\mathbf{C}(f)\mathbf{C}^H(f)+\mathbf{D}(f)\mathbf{D}^H(f)\right)\mathbf{e}_{K,\kappa-3}}+1}\mathrm{d}f\right)^{-2}$, which does not affect the direction of the gradient. Therefore, we simplify the computation by disregarding this factor.

formulated as:

$$\max_{\mathbf{b}} \min_{\substack{4\le l\le K+3,\\ l\neq\kappa}} \mathbf{b}^H \left(\int_{f_0-0.5B}^{f_0+0.5B} \mathbf{C}^H(f)\mathbf{e}_{K,l-3}\mathbf{e}_{K,l-3}^H\mathbf{C}(f)\mathrm{d}f\right)\mathbf{b},$$
$$\text{s.t.: } \mathrm{SNR}_\kappa \ge \mathrm{SNR}_{thr},\ \mathbf{b}^H\mathbf{b} \le P_0. \tag{34}$$

We introduce an auxiliary variable q, which corresponds to a square-root of the minimum receive power, and a new vector variable $\mathbf{y} = [\mathbf{b}^T, q]^T$. Then, (34) can be reformulated into

$$\begin{aligned} &\max_{\mathbf{y}}\ \mathbf{y}^H\mathbf{W}_0\mathbf{y},\\ &\text{s.t.: } \mathbf{y}^H\mathbf{W}_l\mathbf{y} \ge 0,\quad 4\le l\le K+3,\ l\neq\kappa,\\ &\qquad \mathrm{SNR}_\kappa \ge \mathrm{SNR}_{thr},\\ &\qquad \mathbf{y}^H\mathbf{W}_p\mathbf{y} \le P_0, \end{aligned} \tag{35}$$

where the matrices $\mathbf{W}_0$, $\mathbf{W}_l$, and $\mathbf{W}_p$ are given by

$$\mathbf{W}_0 = \mathbf{e}_{4,4}\mathbf{e}_{4,4}^H, \tag{36}$$

$$\mathbf{W}_l = \begin{bmatrix} \left(\int_{f_0-0.5B}^{f_0+0.5B} \mathbf{C}^H(f)\mathbf{e}_{K,l-3}\mathbf{e}_{K,l-3}^H\mathbf{C}(f)\mathrm{d}f\right) & 0 \\ 0 & -1 \end{bmatrix}, \tag{37}$$

$$\mathbf{W}_p = \begin{bmatrix} \mathbf{I}_3 & 0 \\ 0 & 0 \end{bmatrix}. \tag{38}$$

Similarly to the max-sum problem discussed before, we decompose (35) into two subproblems, where the first subproblem corresponds to (35) with relaxed QoS constraint and the second subproblem refers to the QoS constraint and is solved by a gradient based search. The first subproblem is rewritten using trace operators as

$$\begin{aligned} &\min_{\mathbf{Y}}\ \mathrm{tr}\left\{-\mathbf{W}_0\mathbf{Y}\right\},\\ &\text{s.t.: } \mathrm{tr}\left\{-\mathbf{W}_l\mathbf{Y}\right\} \le 0,\quad 4\le l\le K+3,\ l\neq\kappa,\\ &\qquad \mathrm{tr}\left\{\mathbf{W}_p\mathbf{Y}\right\} \le P_0,\quad \mathbf{Y}\succeq 0,\quad \mathrm{rank}\,(\mathbf{Y}) = 1, \end{aligned} \tag{39}$$

where matrix $\mathbf{Y}$ can be expressed as $\mathbf{Y} = \mathbf{y}\mathbf{y}^H$, if $\mathrm{rank}\,(\mathbf{Y}) = 1$ holds. By dropping the rank-1 constraint, this problem becomes a semidefinite program, which can be efficiently solved using the existing methods of convex optimization [32]. Then, the well-known randomization technique [34] is applied in order to obtain a rank-1 solution $\mathbf{y}$ from the matrix $\mathbf{Y}$. The beamforming vector $\mathbf{b}$ is extracted from $\mathbf{y}$ by deleting its last element. Hereafter, the gradient based search is applied, if the QoS requirement for the DR is not fulfilled, using the gradient defined in (32).

C. Convex Transmit Power Approximation

The optimization problems and solutions discussed in Section III-B are well known in the context of far-field communications. With increasing coupling between the devices (in the near-field), the transmit power is more and more influenced by the presence of the receivers, as can be deduced from (19). Hence, the power transfer efficiency can be improved by taking into account this influence in the optimization of the beamforming vector [1]. For this, an iterative algorithm has been proposed, where the total transmit power in (27) and (28) is approximated by a squared L_2-norm for a current iteration, respectively. Employing this approximation, the optimal beamforming vector is calculated, which is used for improving the approximation and updating the solution in the next iteration. For the approximation, we assume that in case of convergence of this algorithm,

$$|\mathbf{b}_i| \approx |\mathbf{b}_{i-1}| \tag{40}$$

holds, where $\mathbf{b}_i = [b_{1,i}, b_{2,i}, b_{3,i}]^T$ denotes the state of the vector $\mathbf{b} = [b_1, b_2, b_3]^T$ at the end of the ith iteration. At first, we approximate the transmit power (19) by

$$\begin{aligned} P_{t,\mathrm{total}} &= \frac{1}{B}\int_{f_0-0.5B}^{f_0+0.5B} |\mathbf{b}_i|^T\,|\mathbf{A}(f)\mathbf{b}_i|\,\mathrm{d}f\\ &\approx \frac{1}{B}\int_{f_0-0.5B}^{f_0+0.5B} |\mathbf{b}_{i-1}|^T\,|\mathbf{A}(f)\mathbf{b}_i|\,\mathrm{d}f, \end{aligned} \tag{41}$$

such that the order of the transmit power with respect to $\mathbf{b}_i$ reduces.[10] Then, we express $|\mathbf{b}_{i-1}|^T$ as

$$|\mathbf{b}_{i-1}|^T = [1,1,1]\,\mathbf{V}_i, \tag{42}$$

using matrix $\mathbf{V}_i$ defined by

$$\mathbf{V}_i = \begin{bmatrix} |b_{1,i-1}| & 0 & 0\\ 0 & |b_{2,i-1}| & 0\\ 0 & 0 & |b_{3,i-1}| \end{bmatrix}. \tag{43}$$

By inserting (42) into (41) and using (43), we obtain

$$\begin{aligned} P_{t,\mathrm{total}} &\approx \frac{1}{B}\int_{f_0-0.5B}^{f_0+0.5B} [1,1,1]\,\mathbf{V}_i\,|\mathbf{A}(f)\mathbf{b}_i|\,\mathrm{d}f\\ &= \frac{1}{B}\int_{f_0-0.5B}^{f_0+0.5B} [1,1,1]\,|\mathbf{V}_i\mathbf{A}(f)\mathbf{b}_i|\,\mathrm{d}f. \end{aligned} \tag{44}$$

Moreover, we define $\mathbf{S}_i(f) = \mathbf{V}_i\mathbf{A}(f)$ and approximate $|\mathbf{V}_i\mathbf{A}(f)\mathbf{b}_i| = |\mathbf{S}_i(f)\mathbf{b}_i|$ from (44) by

$$|\mathbf{S}_i(f)\mathbf{b}_i| \approx |\mathbf{S}_i(f)\mathbf{b}_i| \otimes \left(|\mathbf{S}_i(f)\mathbf{b}_i| \oslash |\mathbf{S}_i(f)\mathbf{b}_{i-1}|\right), \tag{45}$$

where $\otimes$ and $\oslash$ represent element-wise vector multiplication and division, respectively. Hence, by reformulating (45), $|\mathbf{S}_i(f)\mathbf{b}_i|$ can be expressed as

$$|\mathbf{S}_i(f)\mathbf{b}_i| \approx \left(\left|\mathbf{S}_i(f)\mathbf{b}_i \oslash \sqrt{|\mathbf{S}_i(f)\mathbf{b}_{i-1}|}\right|\right)^{②}, \tag{46}$$

where $(\cdot)^{②}$ denotes the element-wise square operator. By multiplying (46) with a vector $[1,1,1]$, the transmit PSD at frequency f can be expressed as a squared L_2-norm using (44):

$$|\mathbf{b}_i|^T\,|\mathbf{A}(f)\mathbf{b}_i| \approx \left\|\mathbf{S}_i(f)\mathbf{b}_i \oslash \sqrt{|\mathbf{S}_i(f)\mathbf{b}_{i-1}|}\right\|_2^2. \tag{47}$$

For the clarity of exposition, we denote $|\mathbf{S}_i(f)\mathbf{b}_{i-1}|$ by vector $\mathbf{g}_i(f) = \left[g_{1,i}(f), g_{2,i}(f), g_{3,i}(f)\right]^T$. Using $\mathbf{g}_i(f)$, the element-wise division in (47) can be formulated as a multiplication with a matrix $\mathbf{Q}_i(f)$, where

$$\mathbf{Q}_i(f) = \begin{bmatrix} \sqrt{g_{1,i}(f)}^{-1} & 0 & 0\\ 0 & \sqrt{g_{2,i}(f)}^{-1} & 0\\ 0 & 0 & \sqrt{g_{3,i}(f)}^{-1} \end{bmatrix}. \tag{48}$$

[10]The order with respect to the complex-valued vector $\mathbf{b}_i$ is larger for $|\mathbf{b}_i|^T\,|\mathbf{A}(f)\mathbf{b}_i|$ than for $|\mathbf{A}(f)\mathbf{b}_i|$.

Then, we obtain

$$\mathbf{S}_i(f)\mathbf{b}_i \oslash \sqrt{|\mathbf{S}_i(f)\mathbf{b}_{i-1}|} = \mathbf{Q}_i(f)\mathbf{S}_i(f)\mathbf{b}_i. \tag{49}$$

Finally, by inserting (49) into (47) and (41), we obtain

$$\begin{aligned} P_{t,\text{total}} &\approx \frac{1}{B}\int_{f_0-0.5B}^{f_0+0.5B} \|\mathbf{Q}_i(f)\mathbf{S}_i(f)\mathbf{b}_i\|_2^2 \,\mathrm{d}f \\ &= \frac{1}{B}\int_{f_0-0.5B}^{f_0+0.5B} \mathbf{b}_i^H \left(\mathbf{Q}_i(f)\mathbf{S}_i(f)\right)^H \left(\mathbf{Q}_i(f)\mathbf{S}_i(f)\right)\mathbf{b}_i \,\mathrm{d}f \\ &= \mathbf{b}_i^H\left(\frac{1}{B}\int_{f_0-0.5B}^{f_0+0.5B} \left(\mathbf{Q}_i(f)\mathbf{S}_i(f)\right)^H \left(\mathbf{Q}_i(f)\mathbf{S}_i(f)\right)\mathrm{d}f\right)\mathbf{b}_i \\ &= \mathbf{b}_i^H\mathbf{P}_i\mathbf{b}_i, \end{aligned} \tag{50}$$

where $\mathbf{P}_i$ is given by

$$\mathbf{P}_i = \frac{1}{B}\int_{f_0-0.5B}^{f_0+0.5B} \left(\mathbf{Q}_i(f)\mathbf{S}_i(f)\right)^H \left(\mathbf{Q}_i(f)\mathbf{S}_i(f)\right)\mathrm{d}f. \tag{51}$$

In case of convergence, the approximations (40), (45), and correspondingly (50) are valid. In the corresponding iterative procedure of Section III-D, the transmit power constraint of (27) and (28) becomes convex in each iteration step. As shown in Section IV, the proposed convex approximation of the transmit power dramatically improves the performance of the SWIPT scheme compared to the far-field approximation based SWIPT under near-field conditions.

D. Iterative Approach

Using the convex transmit power approximation from Section III-C, the two optimization problems (27) and (28) can now be solved more accurately than with the approach of Section III-B. For this, two iterative algorithms are proposed in the following.

1) Max-Sum Problem: In each iteration, the approximation given by (50) is applied to the optimization problem (27):

$$\begin{aligned} \max_{\mathbf{b}_i} \;& \mathbf{b}_i^H\mathbf{W}_{\text{sum}}\mathbf{b}_i, \\ \text{s.t.:} \;& \text{SNR}_\kappa \geq \text{SNR}_{thr}, \\ & \mathbf{b}_i^H\mathbf{P}_i\mathbf{b}_i \leq P. \end{aligned} \tag{52}$$

Here, for the transmit power constraint we utilize P instead of P_0 (like in (29)), since $\mathbf{b}_i^H\mathbf{P}_i\mathbf{b}_i$ represents the transmit power, whereas $\mathbf{b}^H\mathbf{b}$ in (29) represents the voltage variance. Similarly to the procedure according to Section III-B1, (52) is decomposed into two subproblems. The first subproblem is a generalized eigenvalue problem, which is obtained by relaxing the QoS constraint. The second subproblem is related to the QoS constraint and a gradient based search. The generalized eigenvalue problem is solved using a substitution

$$\mathbf{x}_i = \sqrt{\mathbf{P}_i}\mathbf{b}_i, \tag{53}$$

$$\mathbf{b}_i = \sqrt{\mathbf{P}_i}^{-1}\mathbf{x}_i, \tag{54}$$

where $\sqrt{\mathbf{P}_i}$ is calculated via a Cholesky factorization[11] of $\mathbf{P}_i$. An eigenvalue decomposition is applied to the matrix $\left(\sqrt{\mathbf{P}_i}^{-1}\right)^H \mathbf{W}_{\text{sum}} \left(\sqrt{\mathbf{P}_i}^{-1}\right)$ and the (appropriately scaled) eigenvector with the maximum eigenvalue is picked as the optimal solution for $\mathbf{x}_i$. Then, using (54), the optimal beamforming vector $\mathbf{b}_i$ is calculated. If this beamforming vector does not fulfill the QoS constraint, a gradient search is applied based on (32). Then, $\mathbf{b}_i$ replaces $\mathbf{b}_{i-1}$ in the next iteration. The overall optimization algorithm can be described via pseudo code notation given by Algorithm 2. For the starting point $\mathbf{b}_0$ of the algorithm, we select the beamforming vector that corresponds to the solution of the problem (30). Furthermore, we have observed that a number of iterations $N_{\text{iter}} = 5$ seems to provide sufficient accuracy.

[11]Matrix $\mathbf{P}_i$ is obtained via integration of positive definite matrices in (50), which ensures that $\mathbf{P}_i$ is positive definite as well and suitable for the Cholesky factorization.

Algorithm 2 Proposed Solution for Problem (27)

```
Input: b_0, N_iter
for i = 1 to N_iter do
  Calculate P_i using b_{i-1} and (51);
  Perform eigenvalue decomposition of (sqrt(P_i)^{-1})^H W_sum (sqrt(P_i)^{-1});
  Eigenvector with the largest eigenvalue ⇒ x_i;
  b_i = sqrt(P_i)^{-1} x_i;
  Normalize b_i ⇒ P_{t,total} = P;
  Execute Algorithm 1;
  if SNR_κ < SNR_thr then
    Report failure (QoS constraint cannot be satisfied);
    break;
  end if
end for
Output: b_i, b_i^H W_sum b_i.
```

2) Max-Min Problem: Similarly to the previous sections, we decompose the max-min problem (28) into a semidefinite program (by dropping the rank-1 constraint similarly to Section III-B2) and a QoS requirement in each iteration of the algorithm. For this, the transmit power constraint in (39) is modified using matrix $\mathbf{W}_{p,i}$, which depends on $\mathbf{P}_i$:

$$\mathbf{y}_i^H\mathbf{W}_{p,i}\mathbf{y}_i \leq P, \tag{55}$$

where $\mathbf{y}_i$ denotes the state of the vector $\mathbf{y}$ at the end of the ith iteration and matrix $\mathbf{W}_{p,i}$ is given by

$$\mathbf{W}_{p,i} = \begin{bmatrix} \mathbf{P}_i & 0 \\ 0 & 0 \end{bmatrix}. \tag{56}$$

Hence, the semidefinite program in each iteration can be formulated as

$$\begin{aligned} \min_{\mathbf{Y}_i} \;& \text{tr}\left\{-\mathbf{W}_0\mathbf{Y}_i\right\}, \\ \text{s.t.:} \;& \text{tr}\left\{-\mathbf{W}_l\mathbf{Y}_i\right\} \leq 0, \quad 4 \leq l \leq K+3, \; l \neq \kappa, \\ & \text{tr}\left\{\mathbf{W}_{p,i}\mathbf{Y}_i\right\} \leq P, \quad \mathbf{Y}_i \succeq 0, \end{aligned} \tag{57}$$

where the purpose of $\mathbf{Y}_i$ is to approximate $\mathbf{y}_i\mathbf{y}_i^H$. Using convex optimization algorithms [32], (57) is solved resulting in matrix $\mathbf{Y}_i$. Then, using the randomization technique [34] similarly to Section III-B2, an approximation of the solution vector $\mathbf{y}_i$ is obtained. By deleting the last element of this vector, $\mathbf{x}_i$ is extracted. A solution for $\mathbf{b}_i$ is calculated using (54).

Algorithm 3 Proposed Solution for Problem (28)

1: Input: $\mathbf{b}_0$, N_{iter}
2: **for** $i = 1$ **to** N_{iter} **do**
3: Calculate $\mathbf{P}_i$ using $\mathbf{b}_{i-1}$ and (51);
4: Solve (57), apply randomization to $\mathbf{Y}_i \Rightarrow \mathbf{y}_i$;
5: Extract $\mathbf{x}_i$ from $\mathbf{y}_i$ (delete the last element of $\mathbf{y}_i$);
6: $\mathbf{b}_i = \sqrt{\mathbf{P}_i}^{-1}\mathbf{x}_i$;
7: Normalize $\mathbf{b}_i \Rightarrow P_{t,\text{total}} = P$;
8: Execute Algorithm 1;
9: **if** $\text{SNR}_\kappa < \text{SNR}_{thr}$ **then**
10: Report failure (QoS constraint cannot be satisfied);
11: **break**;
12: **end if**
13: **end for**
14: Output: $\mathbf{b}_i$, $\mathbf{y}_i^H \mathbf{W}_0 \mathbf{y}_i$.

If this solution does not satisfy the QoS constraint, the gradient approach is applied. The optimization algorithm can be described via pseudo code notation given by Algorithm 3.

Obviously, the quality of the solutions discussed in Sections III-B2 and III-D2 heavily depends on the accuracy of the utilized randomization technique. According to the literature (cf. [34]), this randomization procedure utilizes a set of random vectors for an approximation of the solution vector based on the semidefinite matrix $\mathbf{Y}$. Furthermore, the accuracy of this method increases with increasing number of generated random vectors. Hence, for a fair comparison between the proposed and the baseline solution of the max-min problem, it is essential to select an identical total number of tested vectors for both schemes. In the proposed solution, the randomization is executed N_{iter} times. Assuming $N_{\text{rand,prop}}$ random vectors in each iteration, the total amount of random vectors generated by the randomization process of the proposed solution is $N_{\text{rand,prop}} N_{\text{iter}}$. Hence, the total number of vectors for the baseline scheme should be $N_{\text{rand,base}} = N_{\text{rand,prop}} N_{\text{iter}}$. With this choice, the performance of the baseline scheme cannot be underestimated. In this work, $N_{\text{rand,prop}} = 200$ and $N_{\text{iter}} = 5$ are selected for the numerical results, such that $N_{\text{rand,base}} = 1000$ results. Both algorithms (Algorithm 2 and 3) may not always be able to find a feasible solution that satisfies the QoS constraint of the original problem. This situation occurs, if the noise power is too large, such that $\text{SNR}_\kappa < \text{SNR}_{thr}, \forall \mathbf{b}$ holds. In such cases, a failure is reported and the respective performance metric $\mathbf{b}_i^H \mathbf{W}_{\text{sum}} \mathbf{b}_i$ or $\mathbf{y}_i^H \mathbf{W}_0 \mathbf{y}_i$ is set to zero.

IV. Numerical Results

In this section, we present numerical results for the MI based SWIPT.

A. System Performance

At first, we assume that all coils have identical system parameters, i.e., $L_t = L_r = L$, $C_t = C_r = C$, and $R_t = R_r = R$. Following the convention of the WPT community [6], we define a factor $F_{m,l} = \frac{2\pi f_0 \overline{M}_{m,l}}{R}$, which corresponds to the product of the quality factor $\frac{2\pi f_0 L}{R}$ and the coupling coefficient $\frac{\overline{M}_{m,l}}{L}$ between coils m and l, respectively. We assume that all receivers are placed at the same distance d from the transmitter, such that the coupling coefficient is identical for all transmitter-receiver links, which means $\overline{M}_{m,l} = \overline{M}$, $m \in \{1,2,3\}$, $l \in \{4,\ldots,K+3\}$. Furthermore, we restrict ourselves to the case $F_{m,l} = F$, $m \in \{1,2,3\}$, $l \in \{4,\ldots,K+3\}$. Since the distances between the receivers may vary, the mutual inductance between them differs from $\overline{M}$. Defining the distance between two adjacent receivers with indices l_1 and l_2 as d_{l_1,l_2}, $\overline{M}_{l_1,l_2}$ can be expressed as

$$\overline{M}_{l_1,l_2} = \overline{M}\left(\frac{d}{d_{l_1,l_2}}\right)^3, \tag{58}$$

because the mutual inductance scales with the third power of the transmission distance [2].

In this work, we assume a random distribution of receiver devices (on a circle around the transmitter) and that their orientation in the three-dimensional space is random. As mentioned earlier, we choose a practically relevant parameter set known from the passive RFID standards and NFC, i.e., a carrier frequency $f_0 = 13.56$ MHz and a bandwidth $B = 14$ kHz. Correspondingly, the quality factor is given by $\frac{2\pi f_0 L}{R} = \frac{f_0}{B} \approx 968$ according to the literature [6]. Furthermore, we select $P = 1$ W and $\text{SNR}_{thr} = 10$ dB. We assume, that in order to satisfy the transmit power constraint, the transmitter adjusts the amplification of the beamforming vector based on the observation of the current in all three transmit circuits. In our simulations, we consider 100 scenarios for each set of system parameters.

We start with a comparison of the performance of the proposed solution (Section III-D1) and that of the baseline scheme (Section III-B1) for the max-sum problem (27), see Fig. 3. We observe that for a large factor F, the sum receive power of the proposed solution is significantly larger than that of the baseline scheme. Furthermore, it can be clearly seen, that the baseline scheme and the proposed solution completely agree for $F < 1$, which is due to the fact that the far-field approximation becomes valid, as explained earlier using (21). Also, we observe that a decrease of the noise variance leads to higher average sum receive powers. The reason is that the gradient search influences the beamforming vector less and less with decreasing noise variance, since the solution of the respective first subproblem (eigenvalue problem) is already close to the solution of the original problem. This is valid because SNR_κ using the selected eigenvector is in many cases already large enough to satisfy the QoS constraint. Interestingly, with increasing number of PRs (from two in Fig. 3a) to four in Fig. 3b)), the performance of both schemes (baseline and proposed) improves substantially, such that average sum receive powers of up to 0.9 W can be reached for $F > 100$. This corresponds to more than 90% power efficiency, if only the WPT is considered.[12] This effect comes from the fact that with increasing number of devices, the number of degrees of freedom increases (the power received at multiple locations is summed up), such that a better power efficiency results

[12]The actual power efficiency is of course somewhat lower due to the losses from the conversion of the received signal into electrical power. However, we assumed $\eta = 1$ in this work, such that these losses are not considered.

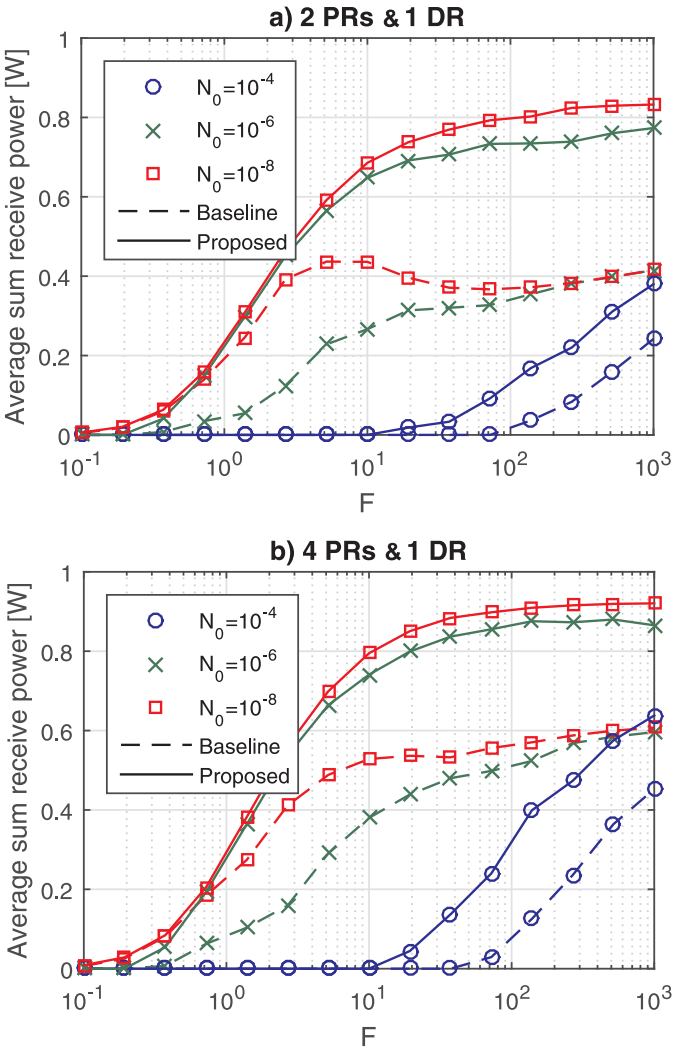

Fig. 3. Average sum receive power obtained from 100 constellations with one data receiver and a) two power receivers or b) four power receivers.

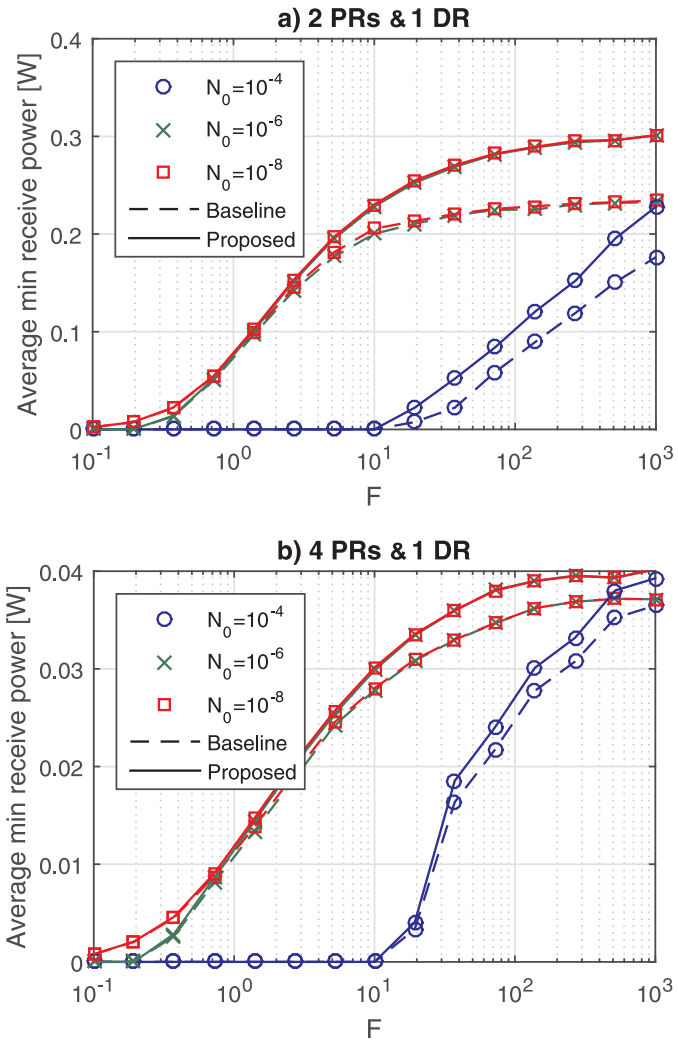

Fig. 4. Average minimum receive power from 100 constellations with one data receiver and a) two power receivers or b) four power receivers.

for a large number of receivers. Moreover, the high power efficiency of the considered MI based SWIPT system is a notable contribution of our work, since it reveals the potential of this scheme.

Fig. 4 shows the performance of the baseline (Section III-B2) and proposed (Section III-D2) solutions for the max-min problem (28). Similarly to Fig. 3, the proposed solution outperforms the baseline scheme in all scenarios, especially for high values of F. Interestingly, we observe that the curves for the proposed solution for $N_0 = 10^{-6}$ V^{2}s and $N_0 = 10^{-8}$ V^{2}s almost completely overlap, which indicates an upper bound in case of vanishing noise. The baseline scheme shows a similar behavior. Unlike in Fig. 3, with increasing number of PRs a dramatic decrease of the figure of merit by almost an order of magnitude is observed. This results from the formulation of the problem (see (35) and (57)), where more PRs impose additional constraints, such that the feasible set shrinks and the performance degrades.

In order to provide a deeper insight into the potential of the proposed magnetic SWIPT system, we present results for both minimum and sum receive powers using the beamforming vectors obtained from the maximization of the sum or the minimum, respectively, see Fig. 5. This means, that we calculate the average minimum receive power using beamforming vectors obtained as solution for the max-sum problem (see Fig. 5a)) and vice versa (see Fig. 5b)). This investigation may help system designers to select the appropriate optimization criterion. For this, we consider $F > 100$, $N_0 = 10^{-6}$ V^{2}s, and two PRs. Interestingly, the baseline solution according to the maximized minimum even outperforms the solution according to the maximized sum in terms of average sum receive power, see Fig. 5b). This indicates the suboptimality of the baseline scheme, since the optimal beamforming solution of the max-sum problem should outperform any other solutions in terms of sum receive power. Furthermore, we observe that the proposed solution is on average $\approx$ 50% worse for the maximized sum compared to the maximized minimum in terms of minimum receive power (Fig. 5a)). On the other hand, the beamforming according to the maximization of the sum is on average only 33% better than the beamforming according to the maximization of the minimum receive power in terms

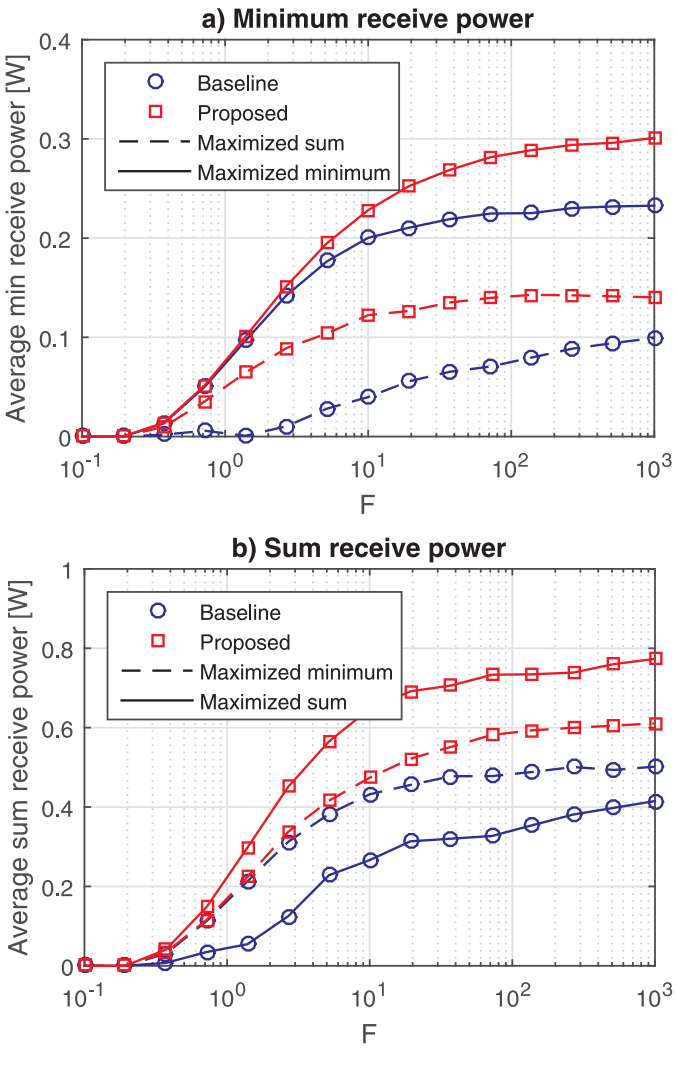

Fig. 5. Average a) minimum or b) sum receive power from 100 constellations with one data receiver and two power receivers for $N_0 = 10^{-6}$ using beamforming solutions from different optimization problems.

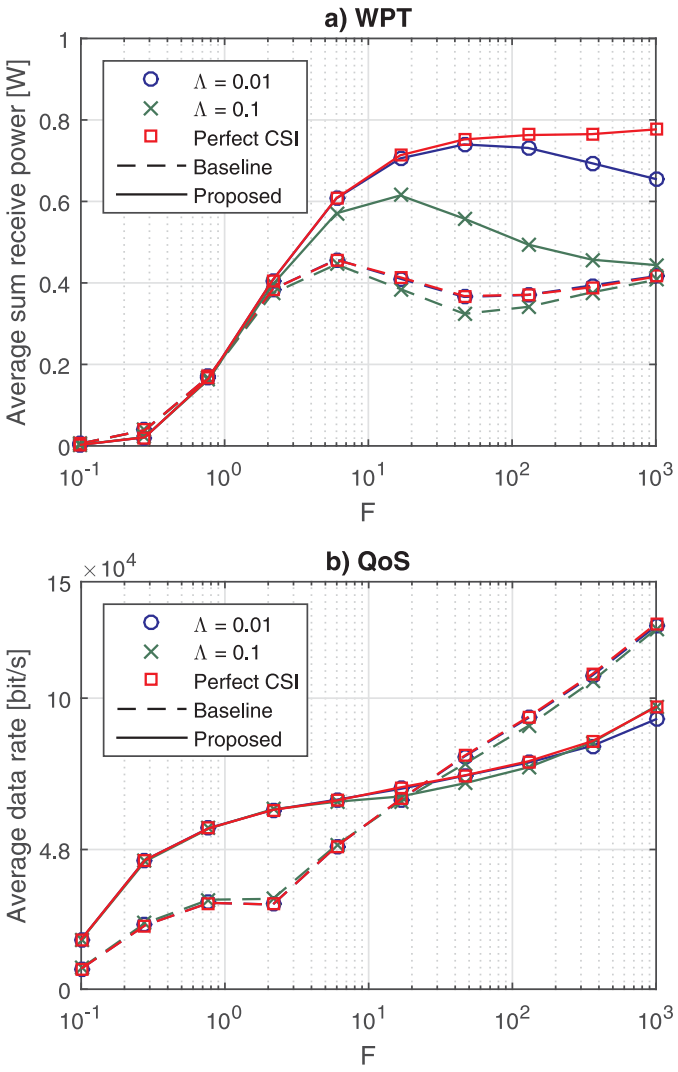

Fig. 6. Average a) sum receive power and b) achievable data rate obtained from 100 constellations with one data receiver, two power receivers, and $N_0 = 10^{-6}$ V^{2}s.

of sum receive power (Fig. 5b)). Of course, more sophisticated fairness based beamforming strategies could provide a trade-off between both optimization metrics. However, this investigation is beyond the scope of this work.

B. Imperfect Channel State Information

The knowledge of the mutual inductance is very important for the optimization of WPT systems [3] and can be acquired either by channel estimation or by distance estimation under the assumption that all other system parameters (coil dimensions, polarization, etc.) are known, cf. [16]. In practice, however, both methods (channel estimation and distance estimation) may not provide the exact value of the mutual inductance due to the noise influence. Correspondingly, this imperfect channel state information (CSI) may lead to a performance degradation. This problem has been already studied in various previous works for RF based SWIPT [19], [35]. In the following, the influence of imperfect CSI on the performance of a magnetic SWIPT system is investigated. For this, we replace the mutual inductance $\overline{M}_{m,l}$ by a Gaussian random variable $\tilde{M}_{m,l}$ with a mean value $\mathcal{E}\{\tilde{M}_{m,l}\} = \overline{M}_{m,l}$ and a standard deviation $\Delta\tilde{M}_{m,l}$. As an additional parameter, we introduce the normalized standard deviation $\Lambda = \frac{\Delta\tilde{M}_{m,l}}{\overline{M}_{m,l}}$. For the following results, the beamforming solution has been obtained for the imperfectly estimated channel, i.e., $\Lambda > 0$. For comparison, we also show results for perfect CSI, i.e., $\Lambda = 0$. Fig. 6a) shows the average sum received power for two power receivers, $N_0 = 10^{-6}$ V^{2}s, and different normalized standard deviations Λ. Obviously, the proposed solution outperforms the baseline scheme in terms of sum receive power even in case of a large standard deviation of the estimated mutual inductances of $\Lambda = 0.1$. Nevertheless, we observe a substantial decrease of the average sum receive power using the proposed solution. A relative decrease of the receive power by almost 45% can be observed for very large values of F. Interestingly, the performance of the baseline scheme does not vary much, such that the receive power decrease is bounded below 6% even for $\Lambda = 0.1$.

Since the imperfect CSI can also affect the fulfillment of the

QoS constraint, we further analyze the QoS for the DR. For a better insight, the obtained values of SNR are mapped onto a maximum achievable data rate via Shannon's capacity formula, $\text{Rate} = B \log_2(1 + \text{SNR})$. Hence, the average data rate would correspond to the expectation value of the achievable rate for the DR, see Fig. 6b). Furthermore, the assumed QoS requirement $\text{SNR}_{thr} = 10$ dB corresponds to ≈48 kbit/s. We observe that the average data rate using the baseline scheme remains mostly unchanged. The proposed solution shows a slight decrease for $\Lambda = 0.01$ and $F > 100$ compared to the case of perfect CSI. Also, a slight decrease is observed for $\Lambda = 0.1$ and $10 \leq F \leq 100$. In general, the baseline scheme outperforms the proposed solution in terms of average data rate only for very large values of F.

C. Coverage

So far, we have assumed that all coils in the system are of equal size. In a practical application, the receiver coils may need to be very small and lightweight, in order to fit into other electronic devices, e.g. smartphones, tablets, etc. On the other hand, the transmitter might be located in an access point, which does not have such restrictions. Hence, in the following, we assume that all receiver coils are implemented as solenoids with $N_r = 1$ turn and $a_r = 2$ cm coil radius. For the transmitter coils, we assume solenoids with $N_t = 200$ turns and $a_t = 20$ cm coil radius. Using the usual dipole approximation of the coil magnet field [13], we obtain the mutual inductance

$$\overline{M} = \mu \pi N_t N_r \frac{a_t^2 a_r^2}{4d^3} \tag{59}$$

between the transmitter coils and any receiver, and

$$\overline{M}_{l_1,l_2} = \mu \pi N_r^2 \frac{a_r^4}{4d_{l_1,l_2}^3} \tag{60}$$

between two receivers l_1 and l_2, respectively, where μ stands for the magnetic permeability. In addition, we calculate the resistance

$$R_t = \rho \frac{2a_t N_t}{a_w^2} \tag{61}$$

of the transmitter coils and the resistance

$$R_r = \rho \frac{2a_r N_r}{a_w^2} \tag{62}$$

of the receiver coils, respectively. Here, $\rho \approx 1.678 \cdot 10^{-2} \Omega \cdot \text{mm}^2/\text{m}$ is the copper resistivity and $a_w = 1$ mm is the wire radius. Using the discussed optimization methods, it is possible to determine the minimum value of the mutual inductance $\overline{M}$, for which the QoS constraint is satisfied and, e.g., the sum receive power is equal to 0.2 W on average. Using (59), the corresponding maximum transmission range d can be deduced via

$$d = \left(\frac{\mu \pi N_t N_r a_t^2 a_r^2}{4\overline{M}} \right)^{1/3}. \tag{63}$$

With four PRs and $N_0 \leq 10^{-6}$ V^{2}s, the maximum transmission range that fulfills the QoS constraint and the sum receive power requirement is $d \approx 50$ cm. If we consider a minimum power requirement of e.g. 0.1 W, the maximum transmission distance with two PRs is $d \approx 40$ cm. Obviously, the coverage of the magnetic SWIPT system is reasonably good for short-distance applications, which makes it a promising candidate for the upcoming Internet-of-Things.

V. Conclusion

In this work, a magnetic induction based SWIPT system has been proposed which utilizes a transmitter with three coils and multiple single coil receivers. From the set of randomly distributed receiver devices, one user (DR) is selected for information reception, whereas the same signal from the transmitter is utilized for the WPT to the remaining users (PRs). Assuming a certain QoS constraint (related to SNR_{thr}), two beamforming problems have been investigated. The first problem (max-sum problem) refers to the maximization of the sum receive power of all PRs. The second problem (max-min problem) refers to the maximization of the minimum receive power among all PRs. Furthermore, the near-field coupling between antennas (coils) has been taken into account, which results in an additional non-convex transmit power constraint. Unfortunately, both problems turn out to be non-convex, such that no globally optimum solution can be obtained. Also, the non-convex transmit power constraint does not allow to apply the well-known beamforming techniques according to the literature. Hence, the max-sum problem has been split into an eigenvalue problem and a QoS problem, and the max-min problem has been split into a semidefinite program and a QoS problem. The respective QoS problems have been solved via a gradient based iterative algorithm. In order to cope with the non-convexity of the transmit power constraint, it has been replaced by an L_2-norm constraint (far-field approximation) for the baseline solution and using a more accurate iterative convex approximation for the proposed solution. In this context, significant performance gains have been observed for the proposed solution in terms of average receive power compared to the baseline scheme, which proves the importance of the mentioned accurate transmit power approximation. Furthermore, with decreasing coupling between coils, we observe a very steep decrease of the received (sum and minimum) power. Similarly, for large noise variances, the received powers are very low. The reason for this behavior is that the optimization focuses more and more on achieving a sufficient level of SNR for the information transmission. Correspondingly, the WPT becomes less relevant.[13] With very weak couplings or large noise variances, it may not always be possible to satisfy the QoS constraint, such that the described optimization problems become infeasible. On the other hand, a high power efficiency of the proposed SWIPT scheme has been observed even for moderate couplings between the coils. Unfortunately, it might not be possible to extend the presented 3D-coil based access point to a transmitter with more than three coils. This is due to the fact that in this case the transmitter coils would not be fully mutually orthogonal anymore, such that the energy

[13] In such cases, a time switching based SWIPT scheme might be preferable, where the power transfer and the information transmission are carried out in disjoint time slots with the optimized duration.

exchange would occur only among the transmitter coils and the performance may even become worse than with three coils. In addition, the angular diversity of the threedimensional space is already completely exploited by the considered 3D-coil, such that possible gains due to additional coils may not justify the increased complexity and cost. However, a more detailed study on an MI transmitter with more than three coils is beyond the scope of this work and remains for future investigations.

REFERENCES

[1] S. Kisseleff, I. F. Akyildiz, and W. Gerstacker, "Beamforming for magnetic induction based wireless power transfer systems with multiple receivers," in *Proc. IEEE Globecom*, Dec. 2015, pp. 1–7.

[2] R. Bansal, "Near-field magnetic communication," *IEEE Antennas Propag. Mag.*, vol. 46, no. 2, pp. 114–115, Apr. 2004.

[3] A. Karalis, J. D. Joannopoulos, and M. Soljačić, "Efficient wireless non-radiative mid-range energy transfer," *Ann. Phys.*, vol. 323, no. 1, pp. 34–48, Jan. 2008.

[4] Z. Sun and I. F. Akyildiz, "Magnetic induction communications for wireless underground sensor networks," *IEEE Trans. Antennas Propag.*, vol. 58, no. 7, pp. 2426–2435, Jul. 2010.

[5] M. C. Domingo, "Magnetic induction for underwater wireless communication networks," *IEEE Trans. Antennas Propag.*, vol. 60, no. 6, pp. 2929–2939, Jun. 2012.

[6] N. Shinohara, *Wireless Power Transfer via Radiowaves*. Hoboken, NJ, USA: Wiley, 2014.

[7] B. W. Flynn and K. Fotopoulou, "Rectifying loose coils: Wireless power transfer in loosely coupled inductive links with lateral and angular misalignment," *IEEE Microw. Mag.*, vol. 14, no. 2, pp. 48–54, Mar. 2013.

[8] Z. Sun, I. F. Akyildiz, S. Kisseleff, and W. Gerstacker, "Increasing the capacity of magnetic induction communications in RF-challenged environments," *IEEE Trans. Commun.*, vol. 61, no. 9, pp. 3943–3952, Sep. 2013.

[9] J. J. Casanova, Z. N. Low, and J. Lin, "A loosely coupled planar wireless power system for multiple receivers," *IEEE Trans. Ind. Electron.*, vol. 56, no. 8, pp. 3060–3068, Aug. 2009.

[10] I.-J. Yoon and H. Ling, "Investigation of near-field wireless power transfer under multiple transmitters," *IEEE Antennas Wireless Propag. Lett.*, vol. 10, pp. 662–665, Jul. 2011.

[11] E. Shamonina, V. A. Kalinin, K. H. Ringhofer, and L. Solymar, "Magneto-inductive waveguide," *Electron. Lett.*, vol. 38, no. 8, pp. 371–373, Apr. 2002.

[12] M. Masihpour and J. I. Agbinya, "Cooperative relay in near field magnetic induction: A new technology for embedded medical communication systems," in *Proc. IB2Com*, Dec. 2010, pp. 1–6.

[13] S. Kisseleff, I. F. Akyildiz, and W. H. Gerstacker, "Throughput of the magnetic induction based wireless underground sensor networks: Key optimization techniques," *IEEE Trans. Commun.*, vol. 62, no. 12, pp. 4426–4439, Dec. 2014.

[14] H. Nguyen, J. I. Agbinya, and J. Devlin, "FPGA-based implementation of multiple modes in near field inductive communication using frequency splitting and MIMO configuration," *IEEE Trans. Circuits Syst. I, Reg. Papers*, vol. 62, no. 1, pp. 302–310, Jan. 2015.

[15] A. Markham and N. Trigoni, "Magneto-inductive networked rescue system (MINERS): Taking sensor networks underground," in *Proc. IEEE IPSN*, Apr. 2012, pp. 317–328.

[16] S. Kisseleff, I. F. Akyildiz, and W. Gerstacker, "Transmitter-side channel estimation in magnetic induction based communication systems," in *Proc. IEEE BlackSeaCom*, May 2014, pp. 16–21.

[17] R. Zhang and C. K. Ho, "MIMO broadcasting for simultaneous wireless information and power transfer," *IEEE Trans. Wireless Commun.*, vol. 12, no. 5, pp. 1989–2001, May 2013.

[18] L. R. Varshney, "Transporting information and energy simultaneously," in *Proc. IEEE Int. Symp. Inf. Theory (ISIT)*, Jul. 2008, pp. 1612–1616.

[19] Z. Xiang and M. Tao, "Robust beamforming for wireless information and power transmission," *IEEE Wireless Commun. Lett.*, vol. 1, no. 4, pp. 372–375, Aug. 2012.

[20] P. Grover and A. Sahai, "Shannon meets Tesla: Wireless information and power transfer," in *Proc. IEEE Int. Symp. Inf. Theory (ISIT)*, Jun. 2010, pp. 2363–2367.

[21] X. Zhou, R. Zhang, and C. K. Ho, "Wireless information and power transfer: Architecture design and rate-energy tradeoff," *IEEE Trans. Commun.*, vol. 61, no. 11, pp. 4754–4767, Nov. 2013.

[22] Y. Zhang, Z. Zhao, and K. Chen, "Frequency splitting analysis of magnetically-coupled resonant wireless power transfer," in *Proc. IEEE ECCE*, Sep. 2013, pp. 2227–2232.

[23] J. I. Agbinya and M. Masihpour, "Power equations and capacity performance of magnetic induction communication systems," *Wireless Pers. Commun.*, vol. 64, no. 4, pp. 831–845, Jun. 2012.

[24] P. Stoica and R. Moses, *Spectral Analysis of Signals*. Upper Saddle River, NJ, USA: Prentice-Hall, 2005.

[25] S. Haykin, *Communication Systems*, 4th ed. Hoboken, NJ, USA: Wiley, 2001.

[26] D. Bernstein, *Matrix Mathematics*. Princeton, NJ, USA: Princeton Univ. Press, 2005.

[27] A. von Meier, *Electric Power Systems: A Conceptual Introduction*. Hoboken, NJ, USA: Wiley, 2015.

[28] H. Akagi, E. H. Watanabe, and M. Aredes, *Instantaneous Power Theory and Applications to Power Conditioning*. Hoboken, NJ, USA: Wiley, Feb. 2007.

[29] N. Tal, Y. Morag, and Y. Levron, "Design of magnetic transmitters with efficient reactive power utilization for inductive communication and wireless power transfer," in *Proc. IEEE Int. Conf. Microw., Commun., Antennas Electron. Syst. (COMCAS)*, Nov. 2015, pp. 1–5.

[30] M. V. Clark, L. J. Greenstein, W. K. Kennedy, and M. Shafi, "Optimum linear diversity receivers for mobile communications," *IEEE Trans. Veh. Technol.*, vol. 43, no. 1, pp. 47–56, Feb. 1994.

[31] Y. W. Liang, R. Schober, and W. Gerstacker, "FIR beamforming for frequency-selective channels with linear equalization," *IEEE Commun. Lett.*, vol. 11, no. 7, pp. 622–624, Jul. 2007.

[32] S. Boyd and L. Vandenberghe, *Convex Optimization*. Cambridge, U.K.: Cambridge Univ. Press, 2004.

[33] D. Tse and P. Viswanath, *Fundamentals Wireless Communication*. Cambridge, U.K.: Cambridge Univ. Press, 2005.

[34] Z.-Q. Luo, W.-K. Ma, A. M.-C. So, Y. Ye, and S. Zhang, "Semidefinite relaxation of quadratic optimization problems," *IEEE Signal Process. Mag.*, vol. 27, no. 3, pp. 20–34, May 2010.

[35] M. R. A. Khandaker and K.-K. Wong, "SWIPT in MISO multicasting systems," *IEEE Wireless Commun. Lett.*, vol. 3, no. 3, pp. 277–280, Jun. 2014.

Steven Kisseleff (S'12) received the Dipl.Ing. degree in information technology with focus on communication engineering from the University of Kaiserslautern, Germany, in 2011. He is currently pursuing the Ph.D. degree in electrical engineering with Friedrich-Alexander-Universität Erlangen-Nürnberg (FAU).

From 2010 to 2011, he was as a Research Assistant with the Fraunhofer Institute of Optronics, System Technologies and Image Exploitation. Since 2011, he has been a Research and Teaching Assistant with the Institute for Digital Communication, FAU, Germany. His research interests include digital communications, wireless sensor networks, wireless power transfer, and magnetic induction based transmissions.

Mr. Kisseleff was a recipient of the Student Travel Grants at the IEEE Wireless Communications and Networking Conference 2013 and the IEEE International Conference on Communications 2014, respectively.

Ian F. Akyildiz (M'86–SM'89–F'96) received the B.S., M.S., and Ph.D. degrees from Friedrich-Alexander-Universität Erlangen-Nürnberg, Germany, in 1978, 1981, and 1984, respectively, all in computer engineering.

He is an Honorary Professor with the School of Electrical Engineering, Universitat Politècnica de Catalunya, Barcelona, Spain, and founded the NaNoNetworking Center in Catalunya (N3Cat). Since 2012, he has been a FiDiPro Professor (Finland Distinguished Professor Program (FiDiPro) supported by the Academy of Finland) with the Department of Communications Engineering, Tampere University of Technology, Finland. He is currently the Ken Byers Chair Professor of Telecommunications with the School of Electrical and Computer Engineering, Georgia Institute of Technology, Atlanta, GA, USA, where he is the Director of the Broadband Wireless Networking Laboratory, and the Chair of the Telecommunications Group.

Dr. Akyildiz has received numerous awards from the IEEE and ACM, as well as the Humboldt Prize in Germany. His current research interests are in wireless underground sensor networks, nanonetworks, and long term evolution advanced networks. He is an Editor-in-Chief of *Computer Networks Journal* (Elsevier), and the founding Editor-in-Chief of the *Ad Hoc Networks Journal* (Elsevier), the *Physical Communication Journal* (Elsevier), and the *Nano Communication Networks Journal* (Elsevier). He is an ACM Fellow (1997).

Wolfgang H. Gerstacker (S'93–M'98–SM'11) received the Dipl.Ing. degree in electrical engineering, and the Dr.Ing. and Habilitation degrees from Friedrich-Alexander-Universität Erlangen-Nürnberg, Erlangen, Germany, in 1991, 1998, and 2004, respectively.

Since 2002, he has been with the Chair of Mobile Communications (now renamed to Institute for Digital Communications) of the Friedrich-Alexander-Universität Erlangen-Nürnberg, and is currently a Professor. His research interests are in the broad area of digital communications and statistical signal processing and include detection, equalization, parameter estimation, MIMO systems and space-time processing, interference management and suppression, resource allocation, relaying, cognitive radio, and sensor networks. He has conducted various projects with partners from industry.

Prof. Gerstacker was a member of the Editorial Board of *EURASIP Journal on Wireless Communications and Networking* from 2004 to 2012. He has served as a member of the Technical Program Committee of various conferences. He has been a Technical Program Co-Chair at the IEEE International Black Sea Conference on Communications and Networking (BlackSeaCom) 2014 and a Co-Chair of the Cooperative Communications, Distributed MIMO and Relaying Track of VTC2013. He is a recipient of several awards, including the Research Award of the German Society for Information Technology (ITG) (2001), the EEEfCOM Innovation Award (2003), the Vodafone Innovation Award (2004), the Best Paper Award of *EURASIP Signal Processing* (2006), and the Mobile Satellite & Positioning Track Paper Award of VTC2011. He has been an Editor for the IEEE TRANSACTIONS ON WIRELESS COMMUNICATIONS since 2012. Furthermore, he is an Area Editor for *Physical Communication* (Elsevier), and has served as a Lead Guest Editor of a Special Issue on Broadband Single-Carrier Transmission Techniques (2013).